

Supporting Information

Microstructural origin of peculiar spectra and excellent luminescence properties of $Y_{10}Ta_4O_{25}:Eu^{3+}$ with fluorite-related structure

Donglei Wei,^{a,b} Xifeng Yang^{*a}, Yushen Liu,^a Hyo Jin Seo^{*b}

¹ School of Electronic and Information Engineering, Changshu Institute of Technology, Changshu, 215500, China

² Department of Physics, Pukyong National University, Busan 48513, Republic of Korea

Figures

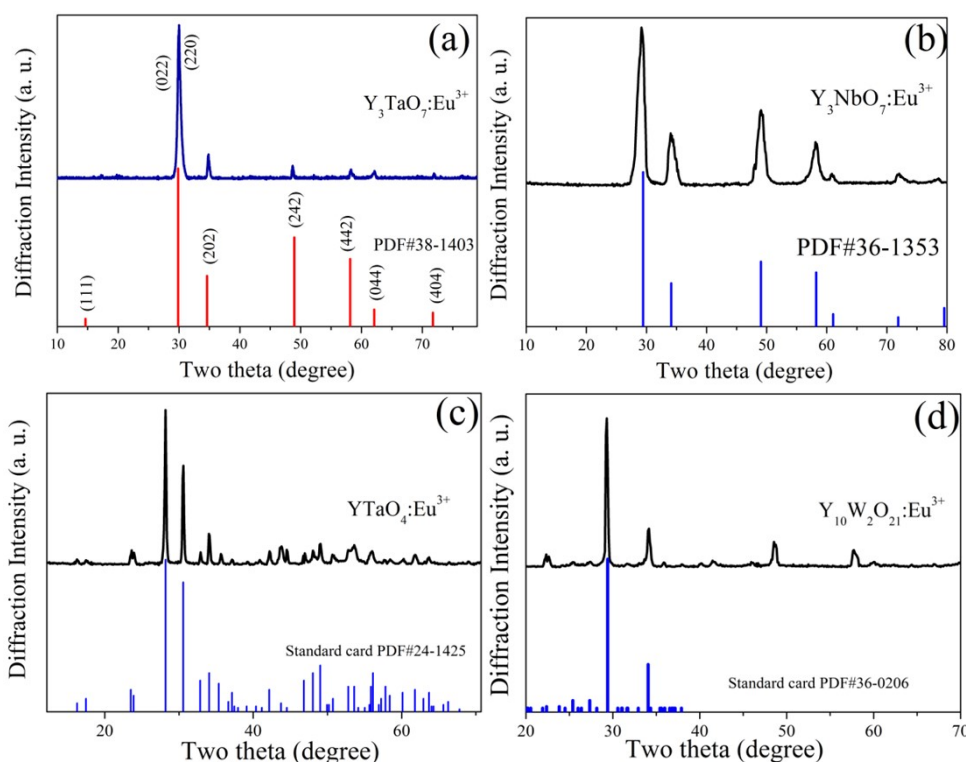


Figure S-1 XRD patterns of the reference samples of $Y_3TaO_7:Eu^{3+}$, $Y_3NbO_7:Eu^{3+}$, $YTaO_4:Eu^{3+}$, $Y_{10}W_2O_{21}:Eu^{3+}$ with the fluorite-related structure. The standard cards were compared with the experimental patterns.

* Corresponding authors: hjseo@pknu.ac.kr (Hyo Jin Seo); xfy@cslg.edu.cn (Xifeng Yang); Tel.: +82-51-629 5568; fax: +82-51-62955494.

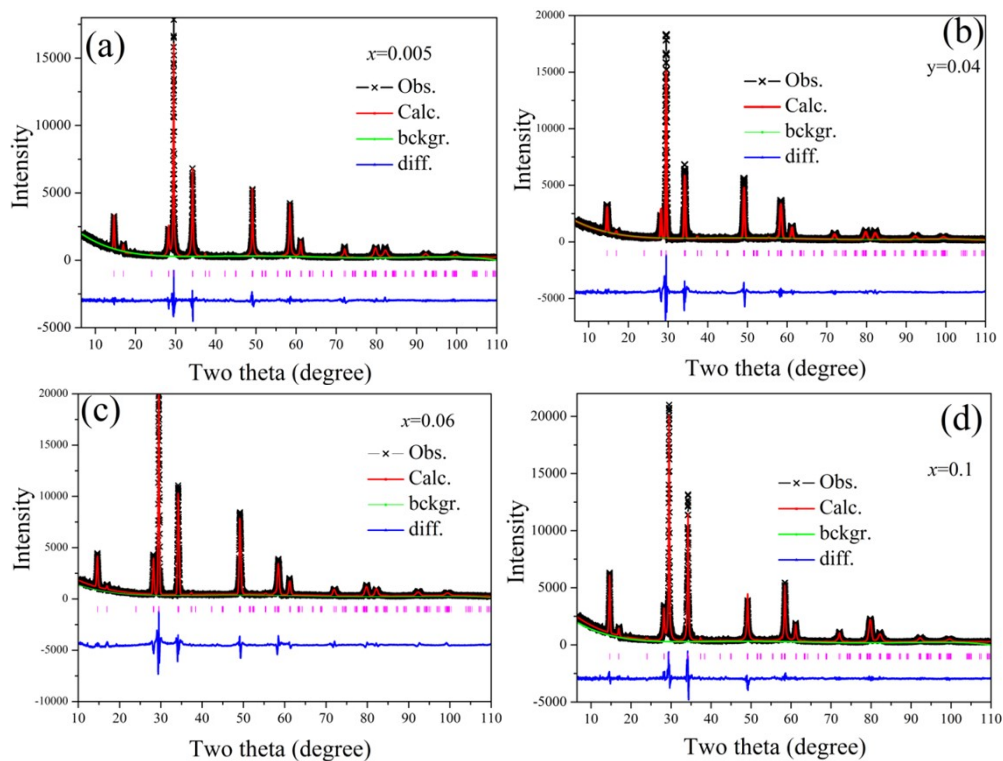


Figure S-2 the representative Rietveld refinements of $Y_{10-10x}Eu_{10x}Ta_4O_{25}$ ceramics with $x=0.005$ (a), $x=0.04$ (b), $x=0.06$ (c) and $x=0.1$ (d).

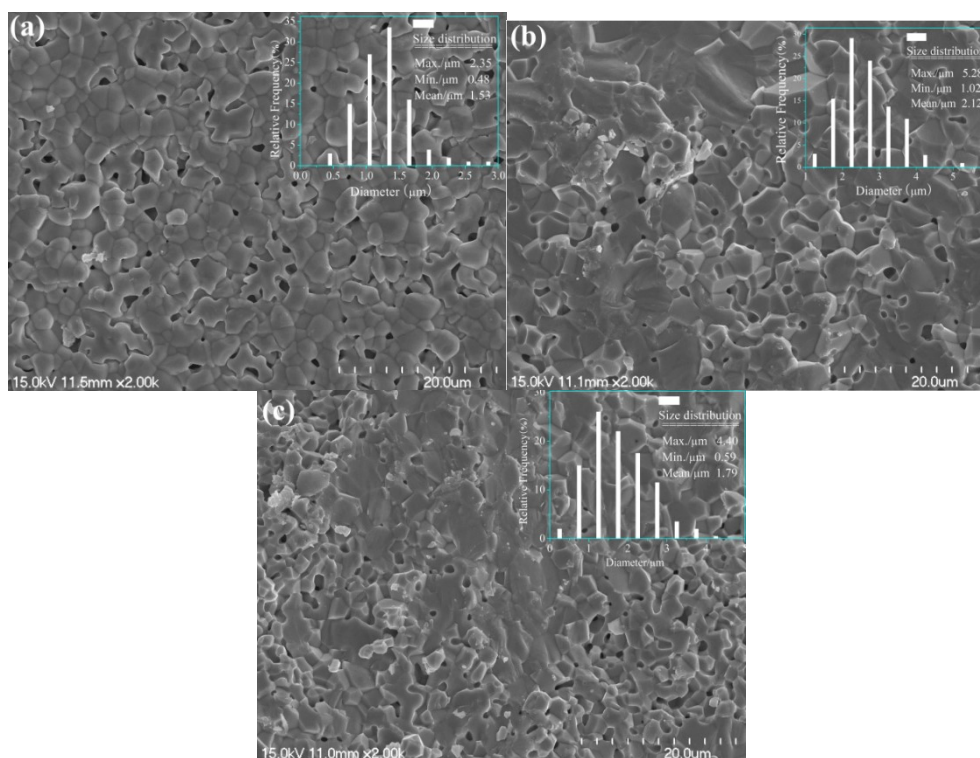


Figure S-3 the representative SEM pictures and the size distribution of the particles of $Y_{10-10x}Eu_{10x}Ta_4O_{25}$ ceramic phosphors with $x=0.005$ (a), $x=0.04$ (b), and $x=0.06$ (c).

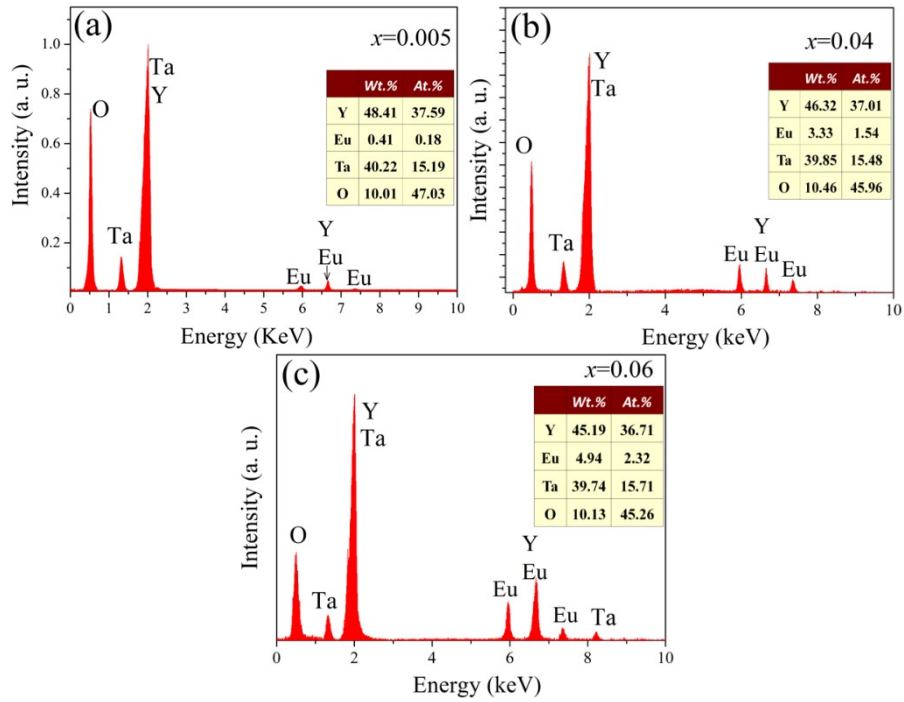


Figure S-4 the representative EDS spectra and the experimental element ratio of $Y_{10-10x}Eu_{10x}Ta_4O_{25}$ with $x=0.005$ (a), $x=0.04$ (b), and $x=0.06$ (c).

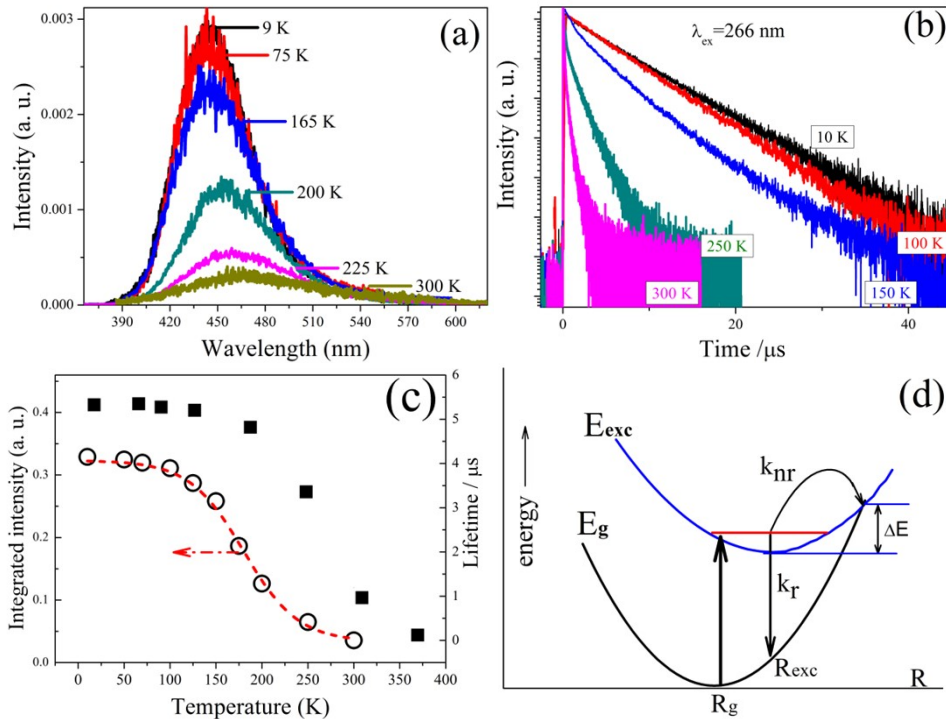


Figure S-5 The intrinsic emission (a), the decay curves (b), temperature-dependent luminescence (c), and the configuration diagram for the ground state (E_g), the excited state (E_{exc}), and electronic transitions (d) of pure $Y_{10}Ta_4O_{25}$ host. R_{exc} and R_g are the equilibrium distances off the excited and ground states, respectively. The excitation was pulsed 266 nm Nd:YAG laser.

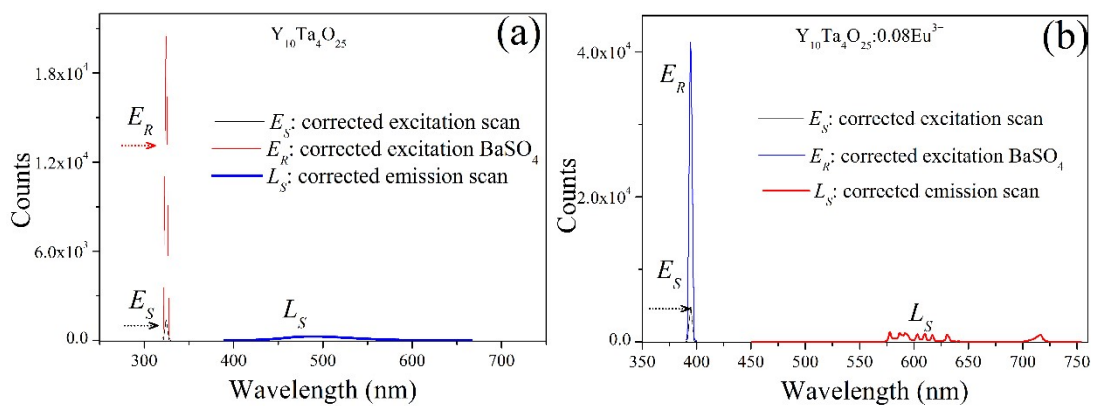


Figure S-6 The corrected excitation line of BaSO₄ and emission spectra of pure (a) and Eu³⁺-doped Y₁₀Ta₄O₂₅ (b) obtained by using an integrating sphere;

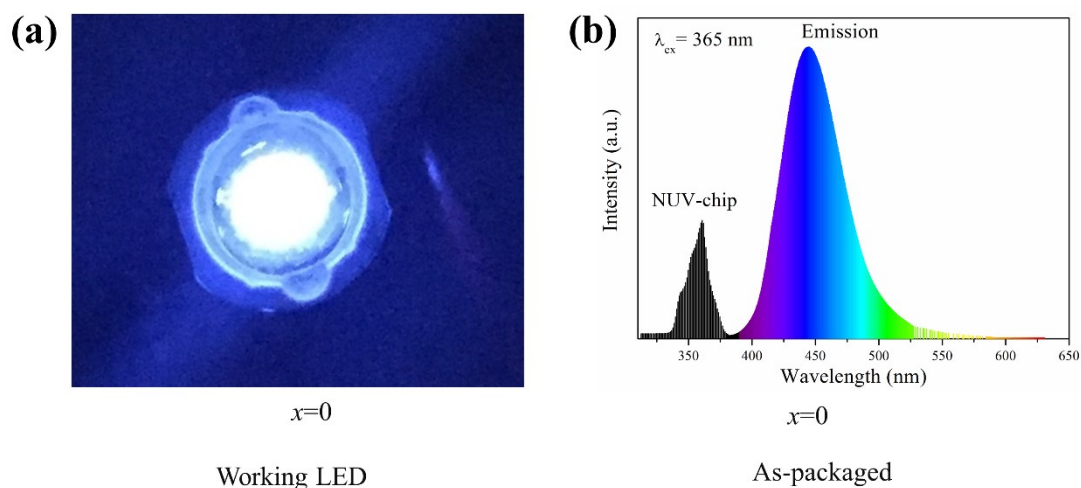


Figure S-7 The experimental LED lighting devices by combining Y₁₀Ta₄O₂₅ with 365 nm chip (a), and its electroluminescence spectrum (b).

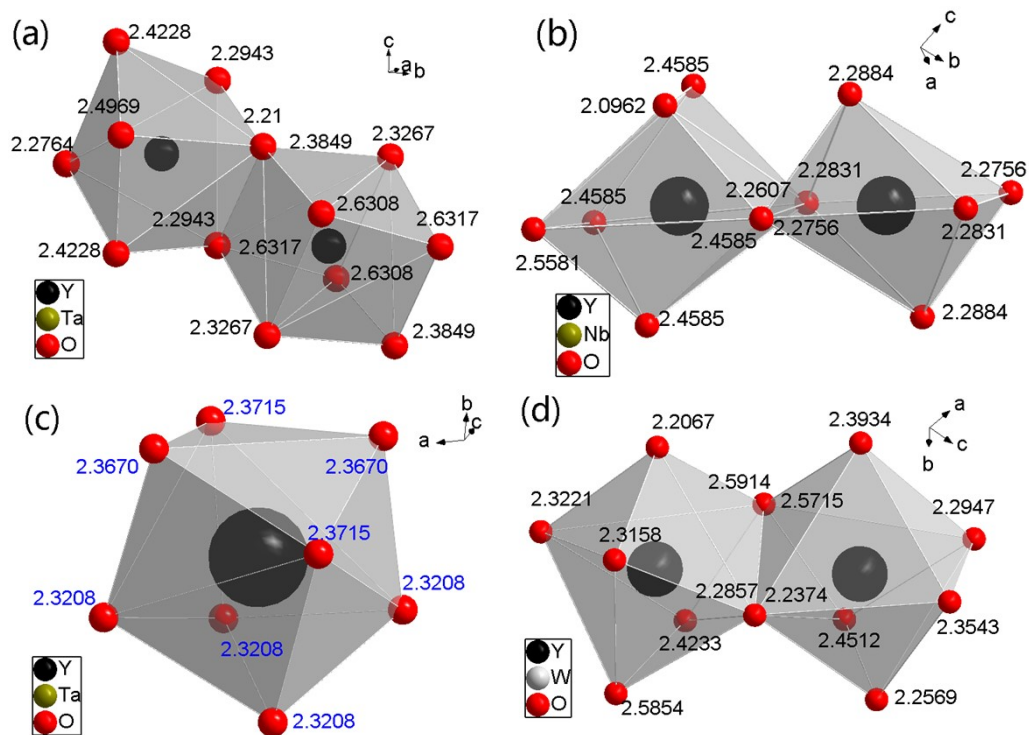


Figure S-8 The local coordination environments of cation sites Y1 and Y2 in the lattices of Y_3TaO_7 (a), Y_3NbO_7 (b), YTaO_4 (c), $\text{Y}_{10}\text{W}_2\text{O}_{21}$ (d). The structures were downloaded from the data base in <https://materialsproject.org>.

Tables

Table S-1 The refined structural parameters of $Y_{10-10x}Eu_{10x}Ta_4O_{25}$ ($x=0.005, 0.04, 0.06, 0.1$) from the Rietveld refinement using X-ray powder diffraction data taken at room temperature.

formula	$x=0.005$	$x=0.04$	$x=0.06$	$x=0.1$
radiation	Cu-K _a	Cu-K _a	Cu-K _a	Cu-K _a
2 θ (°)	5-110	5-110	5-110	5-110
symmetry	orthorhombic	orthorhombic	orthorhombic	orthorhombic
space group#	<i>Cmmm</i> (65)	<i>Cmmm</i> (65)	<i>Cmmm</i> (65)	<i>Cmmm</i> (65)
a/Å	10.4851	10.5542	10.5873	10.6733
b/Å	7.3615	7.3832	7.3881	7.41615
c/Å	3.7327	3.7471	3.8033	3.8565
α /°	90	90	90	90
β /°	90	90	90	90
γ /°	90	90	90	90
Z	2	2	2	2
R _p	0.0838	0.0976	0.0908	0.08218
R _{wp}	0.1149	0.1156	0.1249	0.1122
χ^2	2.21	2.31	2.13	2.53
V/Å ³	288.11782	291.98816	297.49424	305.26046

Table S-2 the Raman mode (cm^{-1}), the average distances of $\text{Y}_{10}\text{Ta}_4\text{O}_{25}:\text{Eu}^{3+}$ compared with the reference samples of $\text{Y}_3\text{TaO}_7:\text{Eu}^{3+}$, $\text{Y}_3\text{NbO}_7:\text{Eu}^{3+}$, $\text{YTaO}_4:\text{Eu}^{3+}$, $\text{Y}_{10}\text{W}_2\text{O}_{21}:\text{Eu}^{3+}$, BaSrMWO_6 and Bi_2WO_6 .

	Raman mode (cm^{-1})	(Y/Eu)-O distances (\AA)		references
		(Y/Eu)1-O	(Y/Eu)2-O	
$\text{Y}_{10}\text{Ta}_4\text{O}_{25}:\text{Eu}^{3+}$	630	2.0123	2.4182	This work
$\text{Y}_3\text{TaO}_7:\text{Eu}^{3+}$	770	2.3453	2.4933	[1]
$\text{Y}_3\text{NbO}_7:\text{Eu}^{3+}$	783	2.3927	2.2824	[2]
$\text{YTaO}_4:\text{Eu}^{3+}$	816	2.3434		[3]
$\text{Y}_{10}\text{W}_2\text{O}_{21}:\text{Eu}^{3+}$	-	2.39	2.3656	
BaSrMWO_6	850	-	-	[4]
Bi_2WO_6	840	-	-	[5]

References

- [1] L. Chen, P. Wu, P. Song, J. Feng, Synthesis, crystal structure and thermophysical properties of $(\text{La}_{1-x}\text{Eu}_x)\text{TaO}_7$ ceramics, *Ceramics International* 44(14) (2018) 16273-16281.
- [2] A. Chesnaud, M.D. Braida, S. Estradé, F. Peiró, A. Tarancón, A. Morata, G. Dezanneau, High-temperature anion and proton conduction in RE_3NbO_7 (RE=La, Gd, Y, Yb, Lu) compounds, *Journal of the European Ceramic Society* 35(11) (2015) 3051-3061.
- [3] J. Wang, Y. Zhou, X. Chong, R. Zhou, J. Feng, Microstructure and thermal properties of a promising thermal barrier coating: YTaO_4 , *Ceramics International* 42(12) (2016) 13876-13881.
- [4] A. Ezzahi, B. Manoun, A. Ider, L. Bih, S. Benmokhtar, M. Azrour, M. Azdouz, J.M. Igartua, P. Lazor, X-ray diffraction and Raman spectroscopy studies of BaSrMWO_6 (M=Ni, Co, Mg) double perovskite oxides, *Journal of Molecular Structure* 985(2) (2011) 339-345.
- [5] M. Mączka, L. Macalik, K. Hermanowicz, L. Kępiński, P. Tomaszewski, Phonon properties of nanosized bismuth layered ferroelectric material— Bi_2WO_6 , *Journal of Raman Spectroscopy* 41(9) (2010) 1059-1066.